

Observation of Electron–Hole Carrier Emission in the Eu^{3+} -Doped Silica Xerogel

Mohammed A. Zaitoun, Taesam Kim,[†] and C. T. Lin*

Department of Chemistry and Biochemistry, Northern Illinois University, DeKalb, Illinois 60115-2862

Received: August 4, 1997; In Final Form: December 15, 1997

The luminescence properties of Eu^{3+} encapsulated in sol–gel-derived optically transparent silica gels were investigated by time-resolved laser spectroscopy. At the xerogel stage, the emission spectra originated mainly from Eu^{2+} at 410 nm, and only a small contribution from Eu^{3+} at 580 nm and electron–hole (e^- – h^+) carrier at 530 nm were observed. It is proposed that in the presence of Eu^{3+} the carriers, e^- – h^+ , were generated during the polycondensation reaction of silica and trapped at the defect sites of sol–gel matrix. The formation of e^- – h^+ carrier was illustrated to be responsible for the surface-assisted reduction of europium ions, where the ejected electrons from the oxygen-associated hole centers react with Eu^{3+} encapsulated in silica gel to produce Eu^{2+} ions.

Introduction

Lanthanide ions are energetically preferred as the trivalent state according to their electron configurations. Many of the spectroscopic investigations were focused on the electronic transitions between f-electron orbitals of trivalent lanthanide ions.¹ Some lanthanide ions, however, can also exist as divalent oxidation state such as Eu^{2+} , Sm^{2+} , and Yb^{2+} . The electronic transitions of divalent ions, $4f^{n-1}5d \rightarrow 4f^n$, are dipole-allowed; they should, in principle, give an intense emission with intensity about 10^6 times those of the f–f transitions of trivalent ions. Because of the large spatial expansion of the 5d wave function, the optical spectra of f–d transitions are quite broad and are very sensitive to the host environments of the divalent ions.² The luminescence intensity of Eu^{2+} is completely quenched in aqueous solution.³ The emission of Eu^{2+} incorporated in a sol–gel-derived SiO_2 glasses was shown to be enhanced about 250 times by codoping 1% of aluminum oxide.²

Eu^{2+} and Sm^{2+} ions have attracted significant attention because they have a great potential for applications in optical communication fields, such as lasers, fiber amplifiers, and optical memories.⁴ Light can promote phototransformation between Eu^{3+} and Eu^{2+} . With the irradiation of a shorter-wavelength UV laser, the Eu^{3+} is excited to a charge-transfer state, by accepting an electron from the surroundings, and is then reduced to Eu^{2+} .⁵ The excited Eu^{2+} plays an important role in the photocatalytic evolution of hydrogen.⁶ The incorporation of Eu^{2+} in $\text{Al}_2\text{O}_3 \cdot \text{SiO}_2$ glass by reducing Eu^{3+} under a flowing gas mixture of H_2 and N_2 has been reported.² The photophysical properties of Eu^{2+} /cryptand complexes⁷ generated by electrochemical reduction of Eu^{3+} and of Eu^{2+} embedded in Vycor glass⁸ have also been published.

In this article, we report an effective process of surface-assisted reduction of Eu^{3+} to form Eu^{2+} in a sol–gel-derived optically transparent silica xerogel. The porous solid matrix in the sol–gel-derived silicates is usually formed by hydrolysis of some desired alkoxide precursors, followed by condensation reaction to yield a polymeric oxo-bridged SiO_2 network.⁹ Upon the formation of SiO_2 network, the defect electrons in the O^{2-}

matrix may be ejected from the creation of an O^- state (or positive hole) during the sol–gel processing. The luminescence properties of electron–hole carrier formed in the Eu^{3+} -encapsulated silica glass will be illustrated. The detection of electron–hole (e^- – h^+) carrier emission could provide the possible mechanism by which the Eu^{2+} may be produced in the silica xerogels.

Experimental Section

Sol–Gel Preparation. Monolithic silica gels were prepared by the acid-catalyzed hydrolysis and polycondensation of tetramethyl orthosilicate (98% TMOS, Aldrich) with deionized water. Ethanol (spectroscopic grade, Aldrich) was added to produce a homogeneous solution. The molar ratio of TMOS: water:ethanol was 1:4:4, and a small amount (about 2 drops) of a 0.04 M HCl was added as a catalyst. Eu^{3+} was introduced during the initial mixing stage by dissolving europium(III) acetate hydrate (99.9%, Aldrich) in the sols prepared above. Based on the initial concentration of the starting solution, a 1×10^{-3} M Eu^{3+} sol was formulated. The resulting solution mixtures were sonicated and were then transferred into a 4.0 mL polystyrene cuvette and covered with parafilm. Gelation occurred in 24 h, and gels were allowed to develop and dry at room temperature until a stabilization of the weight had been completed. The optically transparent monolithic rectangular gels of $2.0 \times 0.43 \times 0.43 \text{ cm}^3$ were obtained and used for the spectroscopic investigations.

Eu^{2+} aqueous solution was prepared by dissolving Eu(II) chloride (99.99%, Aldrich) in deionized water. The absorption spectrum was recorded immediately after sample preparation since Eu^{2+} is not stable in solution under ambient conditions; it completely oxidizes to Eu^{3+} in a few hours.

Laser Spectroscopic Setup. The luminescence spectra and lifetimes of Eu^{3+} encapsulated in xerogel matrix were recorded by using a Q-switched Nd:YAG laser (Continuum, Powerlite 8050, 50 Hz) pumped dye laser (Continuum, ND 6000). The dye laser of Rhodamine 6G was frequency-doubled with a second harmonic generation module to isolate the 280 nm light which was employed as the excitation source. The emission spectra were scanned 500 times and averaged by using an optical multichannel analyzer (EG&G PARC OMA4 with CCD detection). The transient luminescence signal was focused onto a

[†] Visiting scientist from KIGAM, 30, Kajungdong, Yousung, Taejeon, Korea.

* To whom correspondence should be addressed.

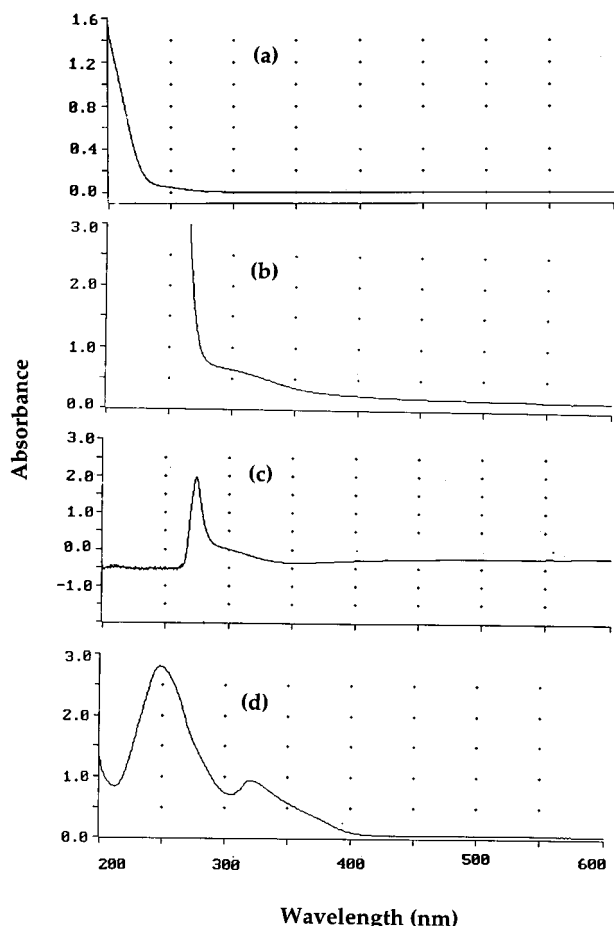


Figure 1. UV-visible spectra: (a) Eu³⁺ in solution, (b) europium ions (i.e., Eu²⁺) in sol-gel at the gelation stage, (c) europium ions (i.e., Eu²⁺) in xerogel using a blank gel as reference, and (d) Eu²⁺ in solution.

monochromator (Shimadzu QV-50) and detected by a 1P28 photomultiplier tube. A fast signal processor (EG&G, model 4400) in combination with a boxcar averager is used to measure the emission decay time. Light absorption spectra of europium cations were recorded on a Cary 3E UV-vis spectrophotometer. The relatively shorter lifetime of Eu²⁺ in gel matrix was measured by a time-correlated single photon counting design lifetime spectrometer (Edinburgh FL900CD).

Results and Discussion

Reduction of Europium Ions in Gel Matrix. Figure 1a shows the absorption spectrum of Eu³⁺ in aqueous solution. The molar extinction coefficient at 280 nm is calculated to be quite small ($\epsilon < 0.6 \text{ M}^{-1} \text{ cm}^{-1}$), which corresponds well to a dipole-forbidden f-f transition.¹⁰ When $1 \times 10^{-3} \text{ M}$ Eu³⁺ is encapsulated in a sol solution, at the wet gel stage, an absorption band extended from 350 to 250 nm is induced as shown in Figure 1b. The spectral feature of the induced absorption of europium ions in xerogel was recorded by using a blank xerogel as reference. The resultant spectrum is displayed in Figure 1c which shows a shoulder band at about 320 nm, and an intense band started from 280 nm and extended toward the shorter wavelength. Note that the spectrum in Figure 1c was sharply cut off at about 260 nm; this is due to the fact that the prepared xerogel is optically transparent only up to about 260 nm.

The question is, what are the oxidation states of europium ions that exist in the xerogel, Eu³⁺, Eu²⁺, or a mixture of both? Figure 1d gives the absorption spectrum of $1 \times 10^{-3} \text{ M}$ Eu²⁺ in aqueous solution. It is noted that the spectrum in Figure 1d

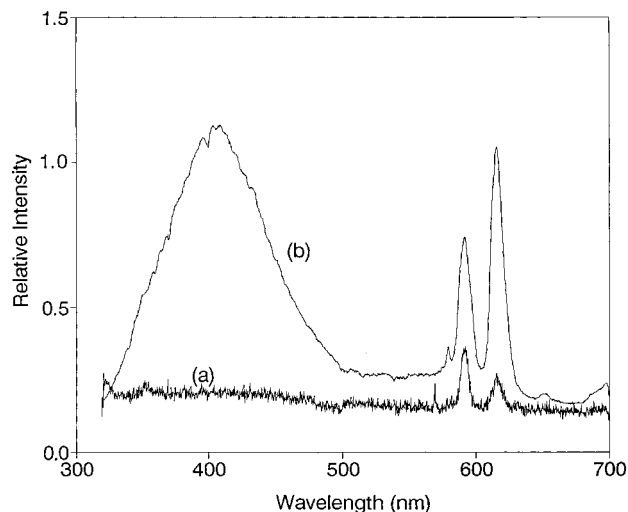


Figure 2. Emission spectra: (a) $1 \times 10^{-3} \text{ M}$ Eu³⁺ in aqueous solution and (b) europium ions (i.e., Eu²⁺ and Eu³⁺) in sol-gel at the gelation stage.

is similar to Figure 1c, which in turn is quite different from Figure 1a. The Eu²⁺ ion absorbs at 320 and 250 nm in Figure 1d, indicating that a large portion of the europium ions exist in gel matrix is the divalent Eu²⁺ as shown in Figure 1c. Since the initial europium ion prepared and encapsulated in sol solution was the trivalent Eu³⁺, it is evident that the Eu³⁺ ion has been effectively reduced to Eu²⁺ ion in xerogel matrix. At 280 nm, the molar extinction coefficient of the Eu²⁺ ion in aqueous solution (Figure 1d) is calculated as $1000 \text{ M}^{-1} \text{ cm}^{-1}$ which is related to a dipole-allowed f-d transition.² Under the same experimental conditions, the molar extinction coefficient at 280 nm in Figure 1c is calculated to be about $650 \text{ M}^{-1} \text{ cm}^{-1}$, suggesting a 65% reduction of Eu³⁺ to Eu²⁺ has taken place in xerogel.

The Eu²⁺ aqueous solution in air is unstable.¹¹ The Eu²⁺ displayed in Figure 1d can be totally oxidized in less than 24 h to form Eu³⁺ as shown in Figure 1a. This result indicates that Eu²⁺ ion can be easily oxidized in air to give Eu³⁺, yet Eu²⁺ is shown to be quite stable in xerogel. Moreover, Eu²⁺ can be further generated from Eu³⁺ via a sol-gel surface-assisted reduction process. The stability of Eu²⁺ in silica xerogel is in part due to its isolation from the oxygen atmosphere in sol-gel matrix. The possible origin and mechanism of surface-assisted reduction of $\text{Eu}^{3+} + \text{e}^- \rightarrow \text{Eu}^{2+}$ will be illustrated in the next section.

Luminescence Properties of Europium Ions Embedded in Sol-Gel Matrix. Lanthanide ions are only weakly luminescent,¹² because they are extremely weak absorbers of electromagnetic radiation. In this study, a large photon flux from a dye laser, about 10 mJ at 280 nm, is used as excitation source to simultaneously excite and detect the luminescence of europium ions of different oxidation states. Figure 2a displays the emission spectrum of Eu³⁺ ions in aqueous solution. The spectral peaks at 590 and 610 nm correspond to $^5\text{D}_0 \rightarrow ^7\text{F}_j$ of Eu³⁺ ion, where $j = 1$ and 2 , respectively.¹³ The weak emission of $^5\text{D}_0 \rightarrow ^7\text{F}_0$ of Eu³⁺ ion at 580 nm is not observed. A sharp peak at 560 nm in Figure 2a is the second order of the laser excitation line (280 nm). The emission band of Eu²⁺ maximum at 410 nm, which does not appear in aqueous solution (Figure 2a) due to quenching by water molecules³ or the instability of Eu²⁺ in air,¹¹ starts to show up in the wet gel and increases gradually till it reaches an optimum intensity at the xerogel stage. Figure 2b shows the emission spectrum of Eu³⁺ encapsulated

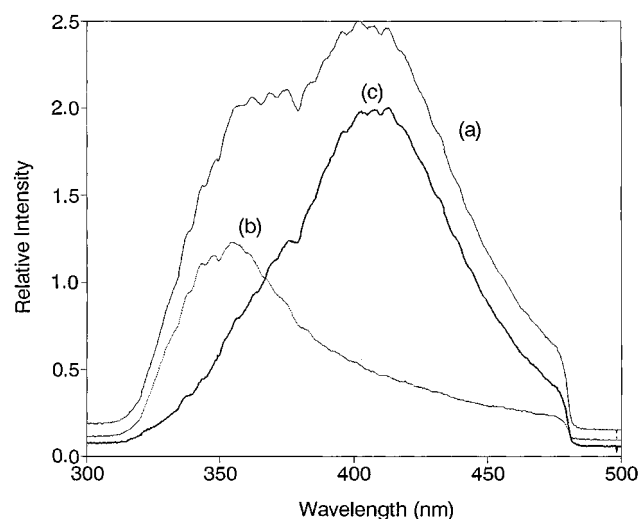


Figure 3. Emission spectra: (a) europium ions (i.e., Eu^{2+}) in xerogel, (b) a blank gel, and (c) the resultant spectrum of (a) - (b).

in gel matrix, during gelation stage but before the xerogel. A broad emission band at 410 nm is clearly observed that may be assigned to the $f-d$ transition of Eu^{2+} ion.¹⁴

The emission peaks of Eu^{3+} in wet gel silicate (Figure 2b) are similar to those in aqueous solution (Figure 2a). The spectral transition, $^5\text{D}_0 \rightarrow ^7\text{F}_0$ of Eu^{3+} ion at 580 nm is now visible in Figure 2b. The hypersensitive transition, $^5\text{D}_0 \rightarrow ^7\text{F}_2$, of Eu^{3+} ion at 610 nm displays a higher emission intensity than the magnetic dipole transition, $^5\text{D}_0 \rightarrow ^7\text{F}_1$, at 590 nm. This picture of spectral intensity distribution (Figure 2b) corresponds to a well-known behavior of Eu^{3+} ion located in a low symmetry site.¹³ In Figure 2a, on the other hand, the band intensity at 590 nm is higher than that at 610 nm since in aqueous solution Eu^{3+} is surrounded by a more symmetric environment. The emission lifetime of Eu^{3+} in aqueous solution and in xerogel is measured as 0.13 and 0.48 ms, respectively. The longer emission lifetime for the emitting species embedded in a rigid matrix is commonly observed¹⁵ as resulting from a slower nonradiative decay process.

The emission lines for the $f-f$ transitions of lanthanide ions (e.g., Eu^{3+}) in a crystalline lattice are generally quite sharp.¹⁶ The homogeneous broadening of the $^5\text{D}_0 \rightarrow ^7\text{F}_j$ transitions in Figure 2b suggests that Eu^{3+} ion is surrounded in a disorder environment of silica gel. The spectral peaks at 580, 590, and 610 nm in Figure 2b are not split and fitted almost to a Gaussian shape, indicating that the xerogel matrix is isotropically distributed. The spectral resolution of an emitting ion is generally limited by the disorder of the host materials. When an Eu^{3+} ion is embedded in the entangled O-Si-O network of xerogel, the spectral features broadened as observed in Figure 2b due to the strong couplings with the phonon and vibration motions of the host lattices.

The thermochemically induced photoluminescence in sol-gel-derived oxide networks has been reported.¹⁷ The blank xerogel displays a broad emission band maximum at 354 nm as shown in Figure 3b which may interfere the true emission spectrum of Eu^{2+} in gel matrix. Figure 3a represents the emission spectrum of europium-doped silica xerogel that displays two spectral bands maximum at 354 and 410 nm. When spectrum b (SiO_2) is subtracted from spectrum a (Eu^{2+} and SiO_2), the resultant spectrum in Figure 3c gives the true emission spectrum of Eu^{2+} ions in xerogel. The emitting species of Eu^{2+} ions shown in Figure 3c should be considered as the products generated from the surface-induced reduction of Eu^{3+} ions

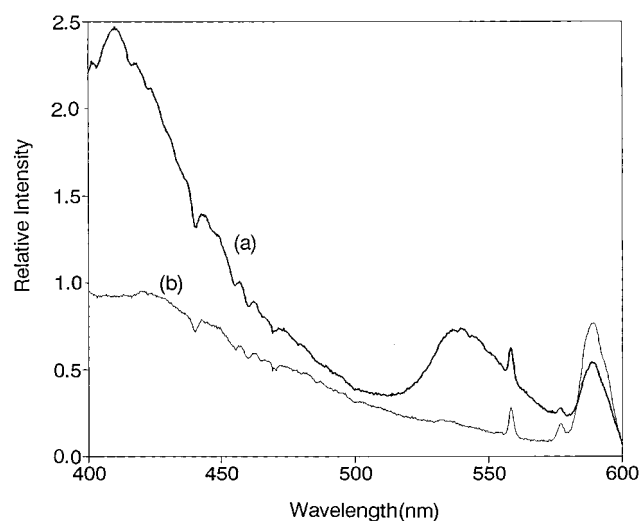


Figure 4. Emission spectra of europium ions (i.e., Eu^{2+} and Eu^{3+}) in xerogels (a) before and (b) after 30 min laser irradiation at 280 nm (50 Hz, 10 mJ).

encapsulated in silica gel. The results agree well with the absorption spectra shown in Figure 1. It is noted that the spectral maximum of a $f-d$ transition is very sensitive to the host environments where Eu^{2+} embedded. The emission lifetime of Eu^{2+} ions monitored at 420 nm of spectrum c is relatively short, about 15 ns, which is quite distinctive from that of the long-lived Eu^{3+} species.

Carriers of Electron-Hole (e^-h^+) Generation in Eu^{3+} -Doped Silica Xerogel. Figure 4a displays the luminescence of Eu^{3+} -doped silica xerogel. The spectrum gives an intense broad band at 410 nm corresponding to Eu^{2+} emission and two weak bands at 580 and 590 nm originated from the $f-f$ transitions of Eu^{3+} ion. Again, the spectral peak at 560 nm is the second order of the excitation laser wavelength, 280 nm. Two observations in Figure 4a require some justifications: (1) the relative emission intensity of $I(\text{Eu}^{2+})/I(\text{Eu}^{3+})$ is very large, indicating that a large portion of encapsulated Eu^{3+} ions has been transformed to Eu^{2+} ions in the xerogel matrix, and (2) for the first time, a broad spectral band at 530 nm has been recorded that may be assigned to the emission of the entrapped electron-hole (e^-h^+) carrier. Upon laser irradiation at 280 nm (50 Hz, 10 mJ), the emission intensity of the e^-h^+ carrier decreases by accompanying an increase of Eu^{3+} and a decrease of Eu^{2+} emission intensity as shown in Figure 4b. After about 30 min of laser irradiation, the e^-h^+ carrier emission disappeared completely. It is important to mention that the effect of laser irradiation on the intensity ratio of $I(\text{Eu}^{2+})/I(\text{Eu}^{3+})$ in spectrum a seems to be reversible. After the irradiated sample was set aside for a few days, the spectral intensity in Figure 4b was able to be restored to that in Figure 4a except that the emission of the electron-hole carrier was not regenerated.

A similar observation on the photoluminescence of electron-hole recombination at 450–550 nm in BaFBr:Eu^{2+} , Eu^{3+} phosphors has been reported.² It was proposed¹⁸ that photo-stimulated luminescence in X-ray storage phosphors takes place when trapped electrons and holes migrate together to form loose clusters around Eu^{2+} and recombine after photostimulation. In the SiO_2 system, the oxygen 2p character of the valence-band edge causes low hole mobility, while the s-like character of the conduction-band edge allows a high electron mobility.¹⁹ At the xerogel stage during sol-gel processing, the silica gel backbone is the O-Si-O network. Silica has a wide band gap (7.6–7.8 eV) and is susceptible to various defects.¹⁹ Among the possible

defects in silica gel matrix are O⁻ states (or positive holes), also called oxygen-associated hole centers.¹⁹ They represent defect electrons in the O²⁻ matrix and a possible form by which it occurs is the self-trapped holes, Si-O⁻-Si. The electron (high mobility) is excited from the valence band to the conduction band, leaving a hole (low mobility) in the valence band.

It is possible that the ejected electrons from the oxygen-associated hole centers react with Eu³⁺ encapsulated in sol-gel matrix to produce Eu²⁺ ions that are stabilized at the cation vacancies by forming Eu²⁺-hole complexes. This reduction process, $\text{Eu}^{3+} + \text{e}^- \rightarrow \text{Eu}^{2+}$, continues to a certain extent during gelation, where Eu²⁺ gives rise to an intense emission band at 410 nm in Figures 2a, 3c, and 4a and absorption spectrum at 320 and 250 nm in Figure 1c. At the final phase of sol-gel densification to become a xerogel, the SiO₂ network forms a rigid structure where the mobility of the ejected electrons is greatly hindered. Furthermore, the Eu³⁺ ions situated around the defect hole centers have been completely reduced to become Eu²⁺. The new picture in the xerogel is a group of Eu²⁺ ions surrounding the generated defect holes. At this moment, further ejected electrons can only be trapped with the positive holes in the field of vacancy of appropriate charge to form bound electron-hole pairs (i.e., excitons) which are stabilized by the Coloumbic interactions. Light excitation of exciton involving transition of the valence electron to exciton state produces emission band at 530 nm in Figure 4a. The lifetime of the e⁻-h⁺ carriers is about 40 μs, which is relatively short as compared to 480 μs of the Eu³⁺ ions.

Upon continuous light irradiation at 280 nm, the defect holes are excited to the conduction band and react with the surrounding Eu²⁺ to regenerate Eu³⁺ ions following the reaction path of $\text{Eu}^{2+} + \text{h}^+ \rightarrow \text{Eu}^{3+}$. This results in the emission intensity decreasing for Eu²⁺ at 410 nm and increasing for Eu³⁺ at 580 and 590 nm as shown in Figure 4b. Laser excitation can anneal the xerogel and detrapp the e⁻-h⁺ carriers. The recombination of e⁻ and h⁺ results in the emission disappearance at 530 nm of the bound electron-hole carriers as illustrated in Figure 4b. It is worth mentioning that, after laser light is removed, the detrapped electrons are highly mobile and can again react with the surrounding Eu³⁺ to form Eu²⁺. The observed spectral intensity in Figure 4a was restored from that in Figure 4b.

An attempt was made to measure the magnetic moment of europium-doped silica xerogel and to estimate quantitatively the ratio of Eu²⁺/Eu³⁺. The electronic ground states of Eu³⁺ and Eu²⁺ are ⁷F₀ and ⁸S_{3/2}, respectively. The theoretical values of magnetic moment of Eu³⁺ and Eu²⁺ based on $\mu_e = g[J(J+1)]^{1/2}\text{BM}$ (bohr magneton) are calculated as 0 and 7.94, respectively, whereas those of the experimental values²⁰ are measured as 3.42 and 7.91, respectively. Magnetic susceptibility (χ_{ac}) of europium-doped silica xerogel was recorded by a Quantum Design Physical Properties Measurement System with an ac field of 15 Oe amplitude and 5 kHz frequency. The results show a well-defined paramagnetic behavior, but the poor signal-to-noise ratio did not yield a meaningful magnetic moment for the europium-doped silica xerogel at this time. To enhance the sensitivity of χ_{ac} measurements, a higher concentration sample of europium-doped silica xerogel is currently under preparation. Furthermore, a Mössbauer spectrometer is also under construction with Prof. Clyde W. Kimball's group for determining the ratio of Eu²⁺/Eu³⁺ encapsulated in sol-gel matrix. The results will be reported in a separate publication.

Conclusion

We have found that, in the presence of Eu³⁺ ions, sol-gel matrix is an effective surface environment for the catalytic

reduction of Eu³⁺ to form Eu²⁺ ions. The Eu²⁺ ions in aqueous solution are unstable in air but become stable inside the oxygen-deficient silica xerogel, where divalent europium is existed as Eu²⁺-hole complexes. For the first time, an emission band at 540 nm was observed for the Eu³⁺ encapsulated silica xerogel and was assigned to originate from the e⁻-h⁺ pairs. The observation of e⁻-h⁺ carriers in xerogel allows us to derive a possible reaction mechanism for the catalytic reduction of Eu³⁺ in sol-gel matrix. The ejected electrons from the oxygen-associated hole centers react with Eu³⁺ encapsulated in xerogel to produce Eu²⁺ ions.

A new field of surface-assisted catalytic reduction of lanthanide ions (and rare-earth ions) has been introduced. The mechanism and efficiency of redox chemistry in silica gel should depend on the types of sol-gel, the conditions of sol-gel preparation, the counterions and redox potentials of the encapsulated lanthanide ions, and trapping and detrapping kinetics of e⁻-h⁺ pairs generated in the sol-gel matrix. Currently, in collaboration with Argonne National Laboratory, electron spin resonance spectroscopy is also used to probe the sol-gel generation of paramagnetic defects in the presence of lanthanides.

Acknowledgment. Financial support from the National Science Foundation Grant CTS-9312875 is acknowledged. T.K. would like to thank Korea Science and Engineering Foundation for a fellowship award. The authors would like to thank Dr. K. Rogacki for performing the ac magnetic susceptibility measurements.

References and Notes

- (1) Reisfeld, R.; Jorgensen, C. K. In *Lasers and Excited States of Rare Earths*; Springer-Verlag: New York, 1993; p 93.
- (2) Nogami, M.; Abe, Y. *Appl. Phys. Lett.* **1996**, 69 (25), 3776.
- (3) Sabbatini, N.; Ciano, M.; Dellont, S.; Bonazzi, A.; Balzani, V. *Chem. Phys. Lett.* **1982**, 90 (4), 265.
- (4) Blasse, G.; Dirksen, G.; Meijerink, A. *Chem. Phys. Lett.* **1990**, 167, 41.
- (5) Kusaba, M.; Nakashima, N.; Kawamaru, W.; Izawa, Y.; Yamanaka, C. *Chem. Phys. Lett.* **1992**, 197 (2), 136.
- (6) Davis, D. D.; Stevenson, K. L.; King, G. K. *Inorg. Chem.* **1977**, 16, 670.
- (7) Sabbatini, N.; Ciano, M.; Dellont, S.; Bonazzi, A.; Boletta, F.; Balzani, V. *J. Phys. Chem.* **1984**, 88, 1534.
- (8) Hazenkamp, M. F.; Blasse, G. *Chem. Mater.* **1990**, 2, 105.
- (9) Brinker, C. J.; Scherer, G. W. *Sol-Gel Science: The Physics and Chemistry of Sol-Gel Processing*; Academic Press: San Diego, CA, 1990.
- (10) Campostrini, R.; Carturan, G.; Ferrari, M.; Montagna, M.; Pilla, O. *J. Mater. Res.* **1992**, 7 (3), 745.
- (11) Yee, E. L.; Gansow, O. A.; Weaver, M. J. *J. Am. Chem. Soc.* **1980**, 102, 2278.
- (12) Horrocks, Jr., W. D.; Schmidt, G. F.; Sudnick, D. R.; Kittrell, C.; Bernheim, R. A. *J. Am. Chem. Soc.* **1977**, 99, 2378.
- (13) (a) Mack, H.; Reisfeld, R.; Avnir, D. *Chem. Phys. Lett.* **1983**, 99, 238. (b) Levy, D.; Mack, H.; Reisfeld, R.; Avnir, D. *Chem. Phys. Lett.* **1984**, 109, 593.
- (14) Haas, Y.; Stein, G.; Tomkiewicz, M. *J. Phys. Chem.* **1970**, 74, 2558.
- (15) (a) Lin, C. T.; Mahloudji, A. M.; Li, L.; Hsiao, M. W. *Chem. Phys. Lett.* **1992**, 8, 193. (b) Horrocks, Jr., W. D.; Sudnick, D. R. *J. Am. Chem. Soc.* **1979**, 101, 334.
- (16) Takahashi, K.; Kohda, K.; Miyahara, J. *J. Lumin.* **1984**, 31&32, 266.
- (17) Yoldas, B. E. *J. Non-Cryst. Solids* **1992**, 147&148, 614.
- (18) Seggern, H. V.; Voigt, T.; Knapfer, W.; Lange, G. *J. Appl. Phys.* **1988**, 64 (3), 1405.
- (19) (a) Freund, F.; Masuda, M. M.; Freund, M. M. *J. Mater. Res.* **1991**, 6 (8), 1619. (b) Mott, N. F. In *Physics of SiO₂ and its Interface*; Pantelides, S. T., Ed.; Pergamon: New York, 1978; p 1.
- (20) (a) Huheey, J. E.; Keiter, E. A.; Keiter, R. L. *Inorganic Chemistry: Principles of Structure and reactivity*, 4th ed.; Harper Collins College Publishers: New York, 1993. (b) Greenwood, N. N.; Earnshaw, A. *Chemistry of the Elements*; Pergamon Press: Elmsford, NY, 1984.